Bull. Mater. Sci., Vol. 37, No. 3, May 2014, pp. 433–439. © Indian Academy of Sciences.

Structural, optical and electrical properties of ZnO thin films prepared by spray pyrolysis: Effect of precursor concentration

F ZAHEDI[1], R S DARIANI[1,*] and S M ROZATI[2]

[1]Department of Physics, Alzahra University, Tehran 1993893973, Iran
[2]Department of Physics, University of Guilan, Rasht 4193833697, Iran

MS received 4 October 2012; revised 13 January 2013

Abstract. **ZnO thin films have been prepared using zinc acetate precursor by spray pyrolytic decomposition of zinc acetate on glass substrates at 450 °C. Effect of precursor concentration on structural and optical properties has been investigated. ZnO films are polycrystalline with (002) plane as preferential orientation. The optical transmission spectrum shows that transmission increases with decrease in the concentration and the maximum transmission in visible region is about 95% for ZnO films prepared with 0·1 M. The direct bandgap value decreases from 3·37 to 3·19 eV, when the precursor concentration increases from 0·1 to 0·4 M. Photoluminescence spectra at room temperature show an ultraviolet (UV) emission at 3·26 eV and two visible emissions at 2·82 and 2·38 eV. Lowest resistivity is obtained at 2·09 Ω cm for 0·3 M. The current–voltage characteristic of the ZnO thin films were measured in dark and under UV illumination. The values of photocurrent and photoresponsivity at 5 V are increased with increase in precursor concentration and reaches to maximum value of 1148 μA and 0·287 A/W, respectively which is correlated to structural properties of ZnO thin films.**

Keywords. **ZnO; thin film; spray pyrolysis; molarity; precursor concentration.**

1. Introduction

ZnO is a promising material for the fabrication of the next generation of optoelectronic devices in the ultraviolet (UV) region and optical or display devices. Its high exciton binding energy (60 meV) can ensure efficient emission at room temperature. ZnO also is a piezoelectric material due to the lack of a centre of symmetry in wurtzite crystal structure. These considerable properties make it suitable for various interesting devices (Cao *et al* 2000; Saito *et al* 2002; Martins *et al* 2004; Hupkes *et al* 2006; Fortunato *et al* 2009; Wu *et al* 2011). Based on these remarkable properties and applications, large efforts have been focused on the fabrication of ZnO thin films and many methods have been employed (Nunes *et al* 1999; Fay *et al* 2005; Xingwen *et al* 2006; Girtan *et al* 2008; Liu *et al* 2011; Rozati *et al* 2011).

In this study, we have prepared ZnO thin films using spray pyrolysis. The electro-optical properties of the film are generally dependent on deposition conditions (Lokhande and Uplane 2000). One of the interesting ZnO applications due to its wide bandgap (3·37 eV) is UV photodetector. The UV photodetector has wide range of applications such as environmental monitoring, solar astronomy, air quality monitoring, accurate measurement of radiation for the treatment of UV-irradiated skin and missile warning system (Basak *et al* 2003; Monroy *et al* 2003; Luo *et al* 2006). Therefore, the investigation of dependence of photoresponse properties of sprayed ZnO thin films on precursor concentration is valuable. In the present work, we have investigated the effect of precursor concentration on structural, optical, electrical properties, dark current, photocurrent and photoresponse of ZnO thin films with the aim to improve the film properties.

2. Experimental

ZnO thin films were deposited by spray pyrolysis method. The experimental home-made set up used for spraying process is given elsewhere (Zahedi and Dariani 2012). The spray solution was prepared by dissolving zinc acetate dehydrate (Merck) in a mixture of deionized water and methanol in the ratio of (1 : 3) in exactly 32 ml for all of the films. A few drops of acetic acid were added to the solution in order to prevent the formation of zinc hydroxide. The concentration of precursor solution was varied from 0·1 to 0·4 M in steps of 0·1 M. Compressed ambient air, which was supplied by an air compressor, was used to atomize the solution. The nozzle–substrate distance was maintained at 28 cm and the substrate temperature was fixed at 450 °C and controlled within ± 10 °C by using a temperature controller unit kept on the metallic hot plate

*Author for correspondence (dariani@alzahra.ac.ir)

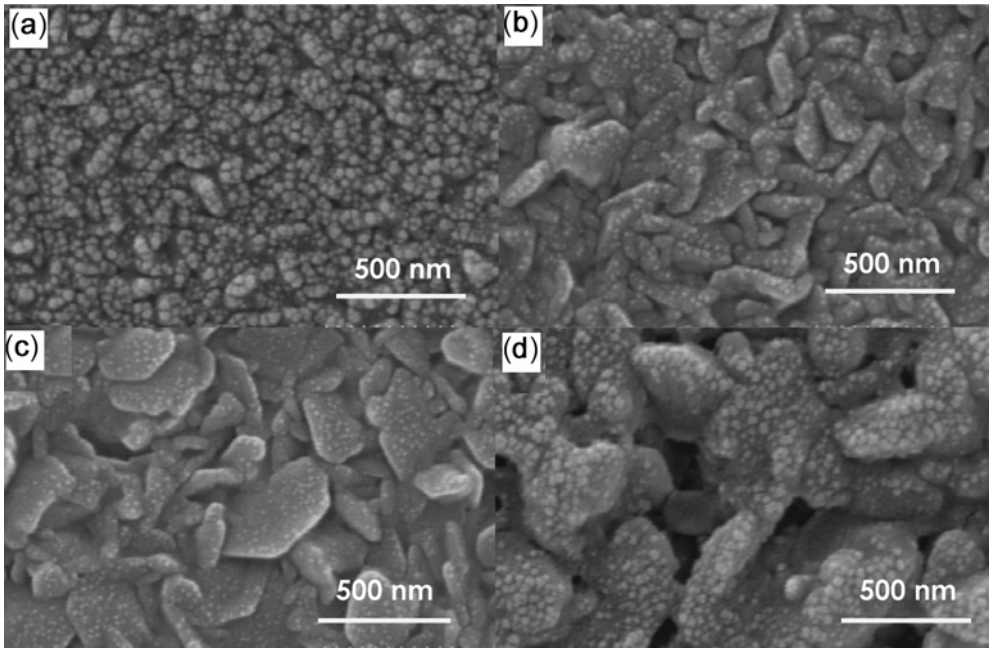

Figure 1. Top view FESEM of ZnO films prepared with precursor concentrations: (**a**) 0·1, (**b**) 0·2, (**c**) 0.3 and (**d**) 0·4 M.

surface. The substrate was soda lime glass which was regularly heated up to the required temperature, before being sprayed on.

The structure of ZnO films was investigated by X-ray diffraction system (XRD; Philips X′ Pert) with CoKα radiation ($\lambda = 0{\cdot}1788$ nm). Surface morphology was examined by a Hitachi S-4166 model field emission scanning electron microscope (FESEM). The thickness of the films was measured by FESEM. The optical transmittance spectrum of the films referenced to the glass was carried out in the wavelength range of 300–800 nm by a high resolution spectrophotometer (Ocean Optics HR4000CG-UV-NIR). Photoluminescence (PL) spectra were measured at room temperature using Cary Eclipse by a source with excitation wavelength of 320 nm. The electrical properties were evaluated by two-probe measurement and current–voltage (*I–V*) method using Sanwa PC5000 and Dual display ESCORT 3146A multimeters. For *I–V* measurements, we used silver paste as electrodes in circle form of about 2 mm diameter separated by 2 mm on ZnO thin films. A Melles Griot He–Cd laser (Series 56) at a wavelength of 325 nm with an optical power of 4 mW was used to excite the samples.

3. Results and discussion

3.1 *Structural properties*

Figure 1 shows the FESEM micrographs were taken to investigate the surface morphology of ZnO films. As seen, ZnO films have uniform density and composed of randomly oriented flake-like grains. The grains are smaller and more elongated in ZnO films prepared with lower precursor concentration. The grain size increases and the shape of the grains become round and hexagonal with increasing precursor concentration. As can be seen in figure 1(c), there are two clearly different crystallite size distributions. Similar results were observed in our previous work (Zahedi *et al* 2013). We suggested that it may be due to the growth mechanism at 450 °C. The porosity of ZnO films were calculated using Lorentz–Lorentz equation (Brinker and Scherer 1975; Yim *et al* 2003; Mirdha and Basak 2006) about 30, 7, 9 and 21%, for 0·1, 0·2, 0·3 and 0·4 M, respectively.

To study the effect of precursor concentration on structural properties of ZnO films, we performed XRD analysis on samples. Figure 2 shows XRD patterns of ZnO films prepared with different precursor concentration in the 20–80° range of 2θ. XRD patterns show that all sprayed films are polycrystalline with hexagonal wurtzite structure. The XRD patterns show diffraction peaks at (002), (101), (102) and (103) for all ZnO films. It is revealed that all sprayed films have a preferred growth orientation along *c*-axis i.e. (002) plane. ZnO usually grows along *c*-axis because the (001) basal plane of ZnO has the lowest surface energy (Zhang *et al* 2004). The intensity of (002) peak is increased as the precursor concentration is increased to 0·4 M. However, in the precursor concentration of 0·3 M, the intensity of (002) diffraction peak decreased in XRD pattern that it can be due to decreasing of film thickness in 0·3 M than 0·2 and 0·4 M. The lattice constants '*a*' and '*c*' for ZnO films

Table 1. Structural properties of ZnO films.

Precursor concentration (M)	Lattice constants (Å)		Crystallite size (nm)	Strain (ε_{zz}) (%)
	a	*c*		
0·1	3·249	5·195	24	–0·23
0·2	3·253	5·205	24	–0·04
0·3	3·254	5·208	24	0·02
0·4	3·256	5·214	24	0·13
Card	3·250	5·207		

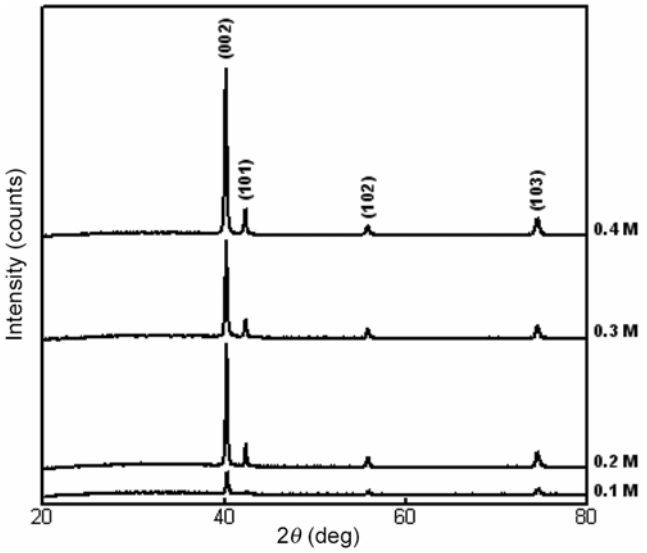

Figure 2. XRD patterns of ZnO films prepared with different concentrations.

with different concentration are calculated using the following equation (Cullity and Stock 2001):

$$\frac{1}{d^2_{(hkl)}} = \frac{4}{3}\left(\frac{h^2+hk+k^2}{a^2}\right)+\frac{l^2}{c^2}.$$

The calculated lattice constants are in good agreement with JCPDS card 36-1451 (table 1).

The *c*-axis strain (ε_{zz}) values are calculated using the following equation (Dutta *et al* 2008):

$$\varepsilon_{zz} = \frac{c-c_0}{c_0}\times 100\%,$$

where '*c*' is the lattice parameter film calculated from the X-ray diffraction data and 'c_0' the unstrained lattice parameter of bulk ZnO. Table 1 gives the variations of strain in terms of precursor concentration. The error bars of measured lattice constants, '*a*' and '*c*', and calculated strain from XRD patterns are 0·003, 0·006 and 30%, respectively. From the data, it can be understood that compressive (negative) strain (ε_{zz}) decreases from 0·1 to 0·2 M and tensile (positive) strain increases from 0·3 to 0·4 M. Therefore, ZnO films prepared from 0·2 and 0·3 M solutions are more relaxed.

Table 1 presents the crystallite size of ZnO films which are estimated using the well known Scherrer formula (Cullity and Stock 2001):

$$D = \frac{0\cdot 9\lambda}{\beta\cos\theta},$$

where λ, θ, and β are the X-ray wavelength (1·78897 Å), Bragg diffraction angle and full width at half maximum of (002) diffraction peak, respectively.

3.2 *Optical properties*

Figure 3 shows the transmission spectrum of sprayed ZnO films with different precursor concentration in the spectral range of 300–800 nm. As seen, all of the films are transparent in visible region, but their UV transmission is low and there is an absorption edge around 380 nm due to bandgap absorption. The transmission spectra of ZnO films show that the transmission decreases with increase in precursor concentration. It can be due to more Zn ion in higher precursor molarity resulting in thicker and consequently, less transparent films (Zaier *et al* 2009). This decreased transmission can be due to increase in roughness with increase in precursor concentration (figure 1) that result in more scattering and therefore decrease in transmission. The maximum transmission is about 95% in visible region for sprayed film with 0·1 M and it decreases to 75% for 0·4 M.

The transmission of ZnO films with different concentrations is higher than transmission of ZnO films with corresponding concentration in our previous work (Zahedi and Dariani 2012). It may be due to the effect of precursor nature including the effect of the salt used in precursor, so that ZnO films with smoother surface morphology and less grain boundary and therefore, more transparent are grown by zinc acetate dehydrate solution than zinc chloride solution.

In order to estimate bandgap, we plotted $(\alpha h\nu)^2$ vs $h\nu$ (figure 4), where α and $h\nu$ are optical absorption coefficient and incident photon energy, respectively. For the direct transition, the optical bandgap energy of ZnO film

was determined using the following equation (Schroder 1998):

$$\alpha h\nu = A(h\nu - E_g)^{1/2},$$

where E_g is the optical bandgap energy and A is a constant. The linearity of the plot of plotted $(\alpha h\nu)^2$ vs $h\nu$ indicates a direct transition (Alver *et al* 2007). The extrapolated values of the optical bandgaps, E_g, are +3·37, +3·22, +3·21 and +3·19 eV for ZnO films produced using 0·1, 0·2, 0·3 and 0·4 M precursor concentrations, respectively. These values of optical bandgap are in good agreement with other reports (Ashour *et al* 2006; Mishra *et al* 2009; Prasada Rao and Santhoshkumar 2009). Therefore, the bandgap of ZnO films decreases with increasing precursor concentration. The decrease in bandgap can be attributed to the variation of strain. Strain changes the inter atomic spacing of semiconductors which affects the energy gap. The compressed lattice will provide a wider bandgap because of the increased repulsion between the oxygen 2*p* and the zinc 4*s* bands. Bandgap decreases for decrease in compressive strain along *c*-axis and decreases for increase in tensile strain (Pankove 1971; Srikant and Clarke 1997; Ghosh *et al* 2004). The thickness of ZnO films prepared from 0·1, 0·2, 0·3 and 0·4 M is 600, 800, 750 and 850 nm, respectively. Therefore, it can be inferred that the decreasing of bandgap is independent of ZnO films thickness. Prasada Rao and Santosh Kumar (2009) suggested that the bandgap of ZnO films does not depend significantly on the thickness. However, Ashour *et al* (2006) reported that the optical bandgap of the sprayed ZnO films influenced with the film thicknesses.

The room temperature photoluminescence (PL) spectra of ZnO films with various precursor concentrations are illustrated in figure 5. The figure shows three main peaks in the spectra for all the films: a sharp and high intensity UV peak around 380 nm (3·26 eV) and two peak emissions at 440 nm (2·82 eV) and 521 nm (2·38 eV) in blue and green regions, respectively. The emission at 380 nm corresponds to the bandgap of ZnO material according to Dong *et al* (2005), this UV emission is assigned to the recombination of bound excitons of ZnO. The origin of the visible emissions has not been conclusively established, and there have been a number of hypotheses proposed for each emission band (Djurisic

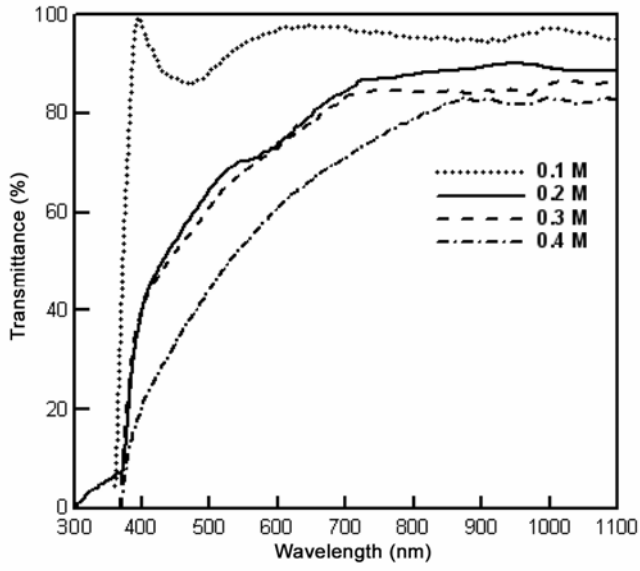

Figure 3. Optical transmission of ZnO films with different concentrations.

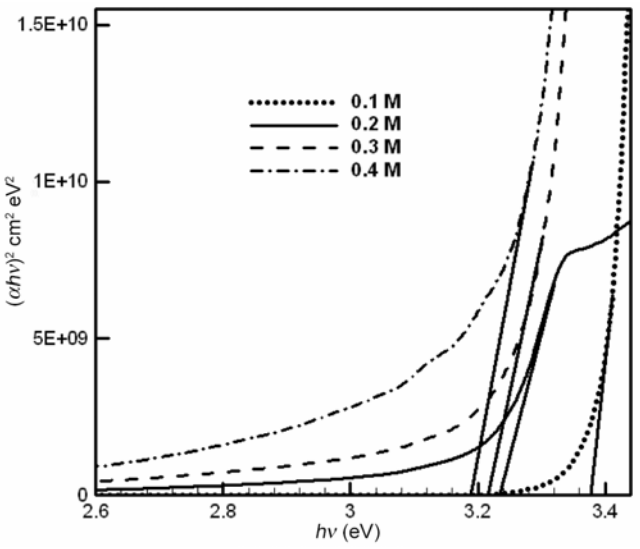

Figure 4. Plot of $(\alpha h\nu)^2$ vs $h\nu$ for ZnO films with different precursor concentrations.

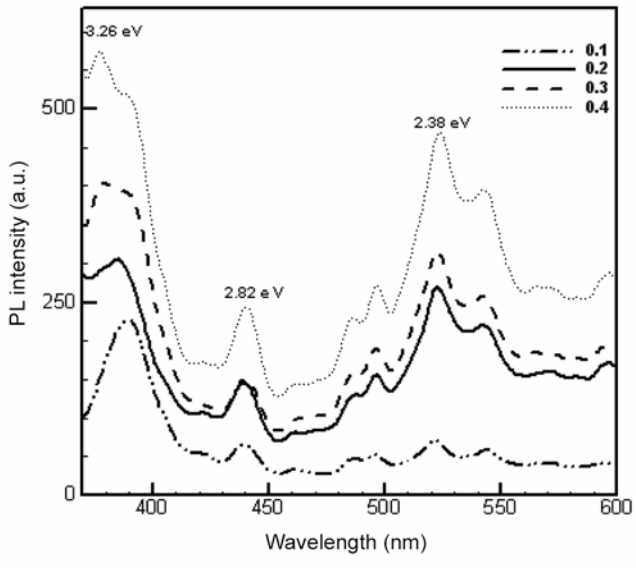

Figure 5. PL spectra for ZnO films with excitation wavelength of 320 nm.

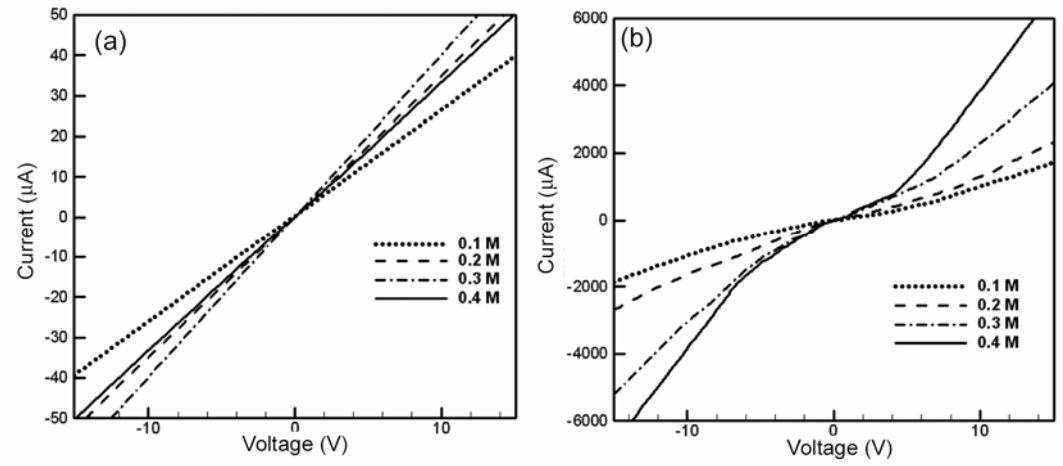

Figure 6. *I–V* characteristics of ZnO films with different concentrations in (**a**) dark and (**b**) UV-illumination.

and Leung 2006). Huang *et al* (2010) suggested that the blue emission peak around 440 nm (2·82 eV) corresponds to the electron transition from the interstitial Zn to the top of the valence band. Vanheusden *et al* (1996) proposed that the green PL emission band is assigned to the oxygen vacancies in ZnO, this luminescence being due to the recombination of photogenerated hole with singly-ionized oxygen vacancies. The effect of precursor concentration in PL spectra is illustrated from the increase in peak intensity with increase in precursor concentration.

3.3 *Electrical properties*

The resistivity of ZnO films with different precursor concentrations was measured at room temperature in dark room (table 2). By increasing the precursor concentration from 0·1 to 0·3 M, the resistivity value decreases from 49·80 to 2·09 Ω·cm and thereafter increases to 3·41 Ω·cm at 0·4 M precursor concentration. This decrease in resistivity can be explained with bigger grains in ZnO films with higher precursor concentration (figure 1). Indeed, when the grain size increases, the electron grain boundary scattering reduces, which results in higher electron mobility and decrease in resistivity (Mridha and Basak 2007). The effect of the precursor on resistivity was investigated by other researchers (Nunes *et al* 2001; Martins *et al* 2004).

Figure 6 shows the measured dark and UV-illumination *I–V* curves of ZnO films. Linear dark *I–V* characteristics confirm the ohmic behaviour of silver contacts for ZnO thin films. The current at a given voltage for the films under UV-illumination is much higher than that under dark condition. This indicates that the UV-illumination increases the production of electron–hole pairs. Therefore, sprayed ZnO thin films are sensitive to UV and can be used in optoelectronic devices such as UV photodetector.

Table 2. Resistivity of ZnO films.

Precursor concentration (M)	Resistivity (Ω·cm)
0·1	49·80
0·2	6·88
0·3	2·09
0·4	3·41

In ZnO thin films, it has been understood that in the dark, oxygen is adsorbed by capturing a free electron from the surface of the *n*-type ZnO, creating a depletion layer near the surface of the film, which reduces the film conductivity. Subsequently, when ZnO films are illuminated by the photon energy more than bandgap energy, the electron–hole pairs are photogenerated and photogenerated holes are drifted by the electric field in the direction of the field extending depletion layer width. These carriers move toward the surface and neutralize the adsorbed oxygen, which causes enhancement of surface conductivity. Consequently, oxygen is desorbed from the surfaces, resulting in an increase in the free carrier concentration and a decrease in the width of the depletion layer (Sharma *et al* 2003).

As seen from figure 6(a), the dark current increases with increase in precursor concentration until 0·3 M and then decreases for films prepared from 0·4 M. As the grain size increases with precursor concentration, the dark conductivity should increase due to increase in carrier concentration (Leary *et al* 1982; Mridha and Basak 2006). Decrease in dark current for film made at 0·4 M may be due to higher porosity than those made at 0·2 and 0·3 M, which causes the diffusion of oxygen gas more readily into the grain boundaries and therefore, the increasing in the amount of adsorbed oxygen at the grain boundaries (Mridha and Basak 2006, 2007). Similar results are reported by Mridha and Basak (2006) for ZnO films with different thicknesses.

Table 3. Photocurrent/dark current ratio, photocurrent and photoresponsivity of ZnO films at 5 V bias and 320 nm illumination.

Precursor concentration		I_{ph}/I_{dark} (micro A)	R (A/w) I_{ph}
0·1	26	344	0·086
0·2	30	508	0·127
0·3	43	866	0·216
0·4	68	1148	0·287

As reported in table 1, the photocurrent ($I_{illuminated} - I_{dark}$) of ZnO films at 5 V increases with precursor concentration. It seems that this result is because of the grain boundaries which are full of traps (defects or impurities) which would capture free carriers. It means that there exists much less grain boundaries in sprayed ZnO films prepared with higher precursor concentration which consists of bigger grain size. Obviously, with the increase in grain size, the photocurrent increases. Mridha and Basak (2006) and Liu *et al* (2007) reported similar results.

The photocurrent ($I_{illuminated} - I_{dark}$) to dark current ratio of ZnO films at 5 V is reported in table 3. One of the important parameters to evaluate a photodetector is the responsivity, R, which is the ratio of the device photocurrent to the incident optical power, which is given by (Liu *et al* 2009):

$$R = \frac{I_{ph}}{P_{inc}},$$

where I_{ph} is the photocurrent and P_{inc} the incident optical power. The responsivity of ZnO films at 5 V is reported in table 3.

Both I_{Ph}/I_{dark} and responsivity increase with increase in precursor concentration. The amounts of reported data in table 1 are comparable with other literature (Mridha *et al* 2006; Liu and Basak 2007). There is a reverse relationship between photocurrent and interelectrode spacing (Salvatori *et al* 1997; Suhail *et al* 2010). Therefore, the amount of I_{ph}, I_{ph}/I_{dark} and responsivity can be increased by decreasing the interelectrode spacing.

The electrical results of sprayed ZnO thin films on low-cost substrate like glass are promising for development of optoelectronic applications such as UV photodetector. Therefore, the photoresponsivity of ZnO films can be improved by optimization of grain size, porosity and ZnO films quality and reducing the interelectrode spacing in sprayed ZnO thin films.

4. Conclusions

In this study, ZnO films are deposited by spray pyrolysis technique. The structural, optical and electrical properties of ZnO thin films were investigated as a function of precursor concentration. The films are poly-crystalline with hexagonal structure with (002) peak as a preferred orientation. The grain size of ZnO films increases with increasing precursor concentration. ZnO film is more relaxed in 0·2 and 0·3 M. The optical transmittance spectrum shows that transmission increases with decreasing precursor concentration and the maximum value of about 95% in the visible region is observed for ZnO film prepared with 0·1 M. A UV emission at 3·26 eV due to exciton recombination and two visible emissions at 2·82 and 2·38 eV that can be attributed to defect emission in ZnO structure have been observed by PL spectra at room temperature. The resistivity value decreases with increasing precursor concentration until 0·3 M from 49·80 to 2·09 Ω·cm and thereafter increases in 0·4 M. The value of photocurrent and photoresponsivity are increased with increasing precursor concentration related to increase in grain size, porosity and quality of ZnO films.

References

Alver U, Kilinc T, Bacaksiz E, Kucukomeroglu T, Nezir S, Mutlu I H and Aslan F 2007 *Thin Solid Films* **515** 3448

Ashour A, Kaid M A, El-Sayed N Z and Ibrahim A A 2006 *Appl. Surf. Sci.* **252** 7844

Basak D, Amin G, Mallik B, Paul G K and Sen S K 2003 *J. Cryst. Growth* **256** 73

Brinker C J and Scherer G W 1975 *Sol–gel science: the physics and chemistry of sol–gel processing* (New York: Academic Press) p. 87

Cao H, Xu J Y, Seelig E W and Chang R P H 2000 *Appl. Phys. Lett.* **76** 2997

Cullity B D and Stock S R 2001 *Elements of X-ray diffraction* (New Jersey: Prentice Hall)

Djurisic A B and Leung Y H 2006 *Small* **2** 944

Dong L, Liu Y C, Tong Y H and Xiao Z Y 2005 *J. Coll. Interf. Sci.* **283** 380

Dutta M, Mridha S and Basak D 2008 *Appl. Surf. Sci.* **254** 2743

Fay S, Kroll U, Bucher C, Vallat-Sauvain E and Shah A 2005 *Sol. Energy Mater. Sol. Cells* **86** 385

Fortunato E, Goncalves A, Pimentel A, Barquinha P, Goncalves G, Pereira L, Ferreira I and Martins R 2009 *Appl. Phys. A* **96** 197

Ghosh R, Basak D and Fujihara S 2004 *J. Appl. Phys.* **96** 2689

Girtan M, Rusu G G, Dabos-Seignon S and Rusu M 2008 *Appl. Surf. Sci.* **254** 4179

Huang B, He G and Yang H 2010 *Physica B* **405** 4101

Hupkes J, Rech B, Kluth O, Repmann T, Zwayagardt B, Muller J, Drese R and Wutting M 2006 *Sol. Energy Mater. Sol. Cells* **90** 3054

Leary D J, Bornes J O and Jordon A G 1982 *J. Electrochem. Soc.* **129** 1382

Liu A, Zhang J and Wang Q 2011 *Chem. Eng. Comm.* **198** 494

Liu C Y, Zhang B P, Lu W, Binh N T, Wakatsuki K, Segawa Y and Mu R 2009 *J. Mater. Sci.* **20** 197

Liu J M, Xia Y B, Wanga L J, Su Q F and Shi W M 2007 *J. Cryst. Growth* **300** 353
Lokhande B J and Uplane M D 2000 *Appl. Surf. Sci.* **167** 243
Luo L, Zhang Y, Mao S S and Lin L 2006 *Sens. Actuators A* **127** 201
Martins R, Fortunato E, Nunes P, Ferreira I and Marques A 2004 *J. Appl. Phys.* **96** 1398
Mishra D, Dubey K C, Shukla R K, Srivastava A and Srivastava A 2009 *Sens. Trans. J.* **105** 119
Monroy E, Omnes F and Calle F 2003 *Semicond. Sci. Tech.* **18** 33
Mridha S and Basak D 2006 *Chem. Phys. Lett.* **427** 62
Mridha S and Basak D 2007 *Mater. Res. Bull.* **42** 875
Nunes P, Fortunato E, Lopes A and Martins R 2001 *Int. J. Inorg. Mater.* **3** 1129
Nunes P, Malik A, Fernandes B, Fortunato E, Vilarinho P and Martins R 1999 *Vacuum* **52** 45
Pankove J I 1971 *Optical processes in semiconductors* (New York: Dover Publication) Ch. 2, p. 22
Prasada Rao T and Santhoshkumar M C 2009 *Appl. Surf. Sci.* **255** 4579
Rozati S M, Zarenejad F and Memarian N 2011 *Thin Solid Films* **520** 1259
Saito N, Haneda H, Sekiguchi T, Ohashi N, Sakaguchi I and Koumoto K 2002 *Adv. Mater.* **14** 418
Salvatori S, Pace E, Rossi M C and Galluzzi F 1997 *Diam. Relat. Mater.* **6** 361
Schroder D K 1998 *Semiconductor material and device characterization* (New York: Wiley)
Sharma P, Sreenivas K and Rao K V 2003 *J. Appl. Phys.* **93** 3963
Srikant V and Clarke D R 1997 *J. Appl. Phys.* **81** 6357
Suhail A M, Hassan E K, Ahmed S S and Alnoori M K M 2010 *J. Electr. Dev.* **8** 268
Vanheusden K, Warren W L, Seager C H, Tallant D R, Voigt J A and Gnade B E 1996 *J. Appl. Phys.* **79** 7983
Wu Y, Girgis E, Strom V, Voit W, Belova L and Rao K V 2011 *Phys. Status Solidi A* **208** 206
Xingwen Z, Yongqiang L, Ye L, Yingwei L and Yiben X 2006 *Vacuum* **81** 502
Yim J H *et al* 2003 *Mat. Res. Soc. Symp. Proc.* **766** E8.10.1
Zahedi F and Dariani R S 2012 *Thin Solid Films* **520** 2132
Zahedi F, Dariani R S and Rozati S M 2013 *Mater. Sci. Semicond. Process.* **16** 245
Zaier A, OumElaz F, Lakfif F, Kabir A, Boudjadar S and Aida M S 2009 *Mater. Sci. Semicond. Process.* **12** 207
Zhang H Z, Sun X C, Wang R M and Yu D P 2004 *J. Cryst. Growth* **269** 464